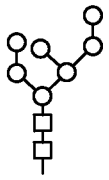
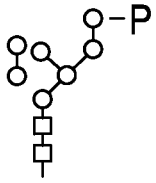
Fig. 1A

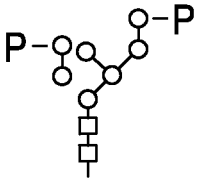
Structure and Receptor Affinity for High Mannose and Phosphorylated Oligosaccharides



Non-phosporylated High Mannose N-glycan:



Mono-M6P N-glycan:
Lower affinity for CI-MPR
(K_n ~ 7000 nM)

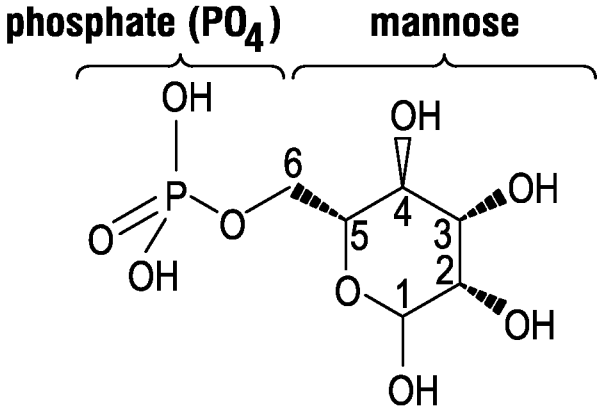


Bis-M6P N-glycan:
High Affinity for CI-MPR
(K_n = 2 nM)

Fig. 1B

Chemical Structure of Mannose 6-phosphate

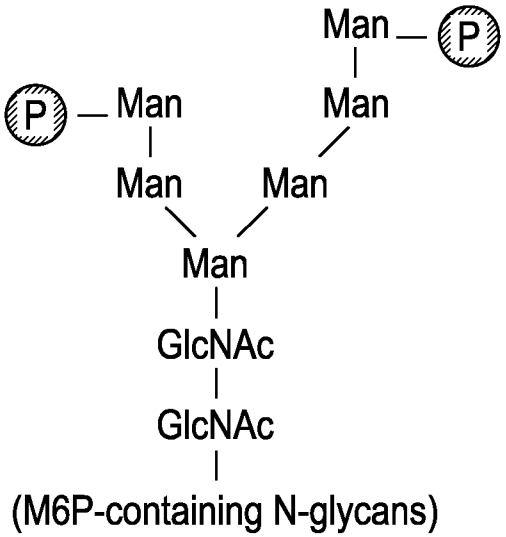
Mannose 6-phrosphate (M6P)



Comparison of Productive and Non-Productive Targeting Glycan Specific Receptors

Productive

Productive Drug Targeting



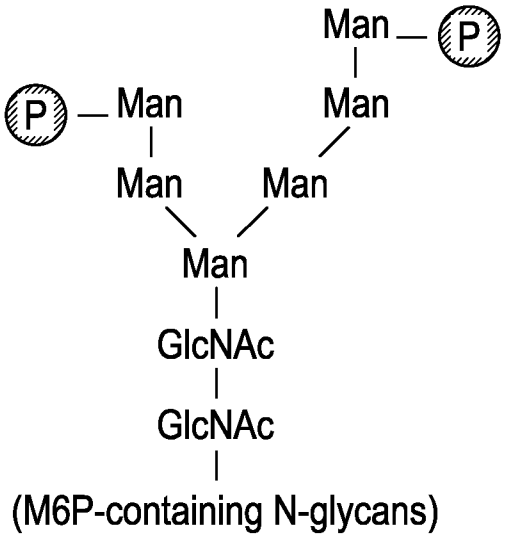
(M6P-containing N-glycans)

Target tissues
(M6P-R; heart, skeletal muscles, diaphragm, etc.)

Fig. 2A

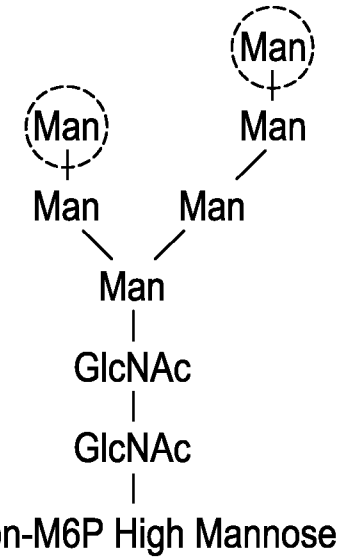
Non-Productive

Non-Productive Drug Clearance



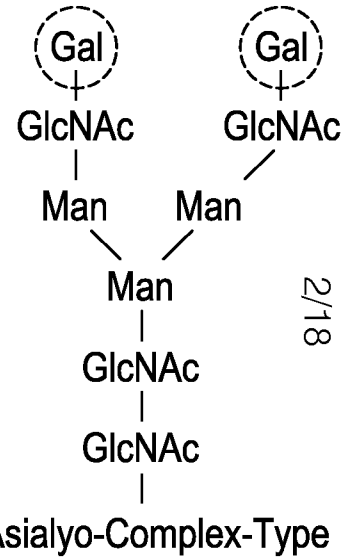
(M6P-containing N-glycans)

Non-Target tissues
(M6P-R; liver, spleen, gut, etc.)



(Non-M6P High Mannose N-glycans)

Non-Target tissues
(Mannose Receptors; liver, spleen)



(Asialyo-Complex-Type N-glycans)

Non-Target tissues
(ASGP-R; liver)

Fig. 2B

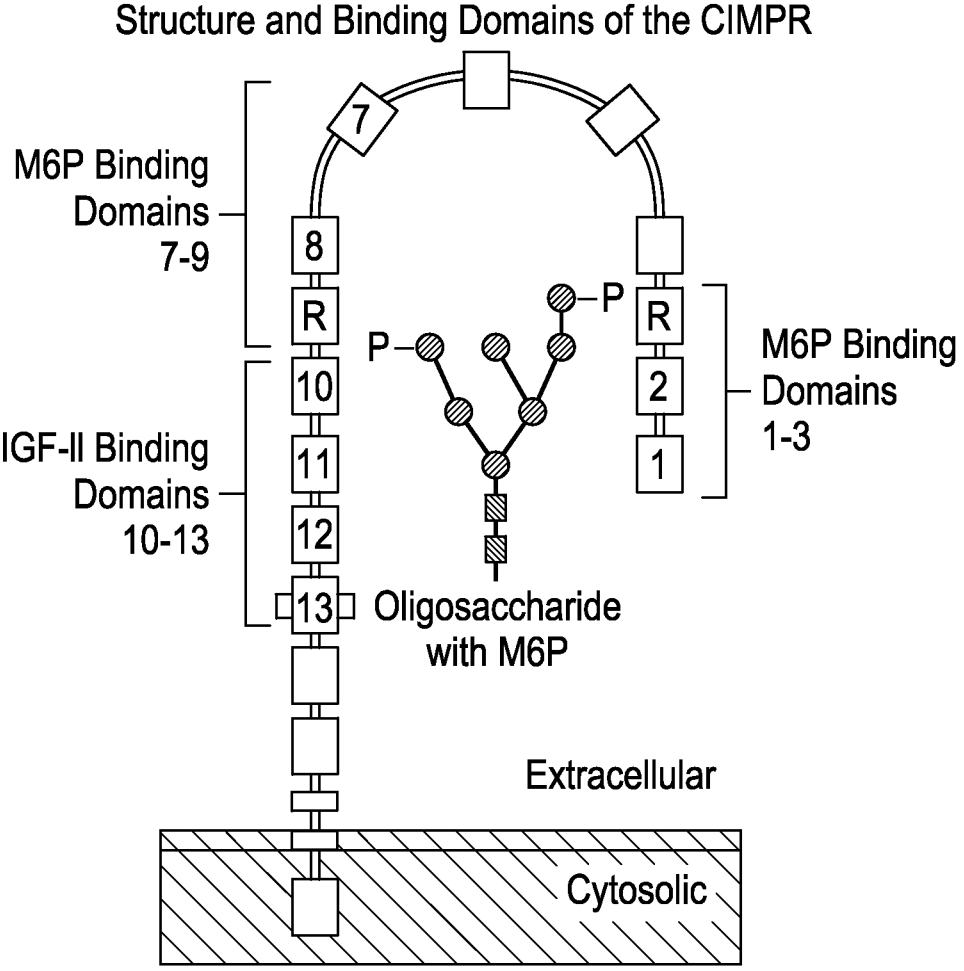


Fig. 3A

Ligands; Affinity and In Vivo Location of Three Glycoprotein Receptors

Ligand	Receptor	Affinity (nmolar)	Location
Bis-Phosphoylated Glycan	CIMPR	2	All Cells
Mono-Phosphorylated Glycan		7,000	
High Mannose Glycan	Mannose Receptor	20[b]	Macrophages Dendritic Cells
De-sialylated Complex Glycan	Asialyoglycoprotein Receptor	7[c]	Hepatocytes

Reference: [a]Tong *et al* 1989; [b]Taylor *et al* 1992; [c]Schwartz *et al* 1981

Fig. 3B

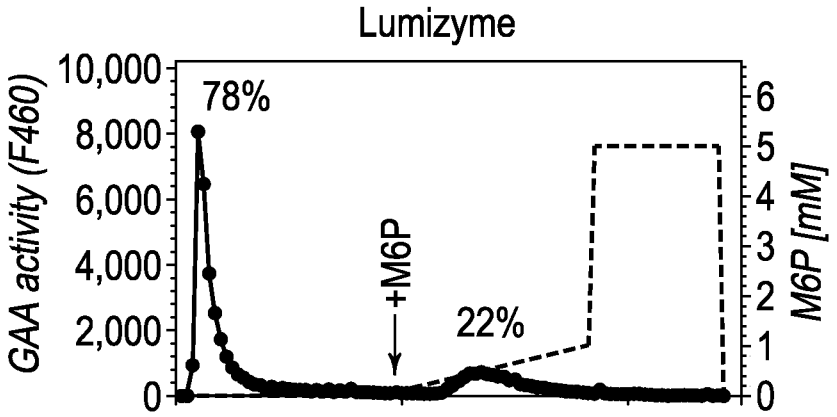

Lumizyme
GAA activity (F460)
10,000
8,000
6,000
4,000
2,000
0
78%
+M6P
22%
6
5
4
3
2
1
0
M6P [mM]

Fig. 4A

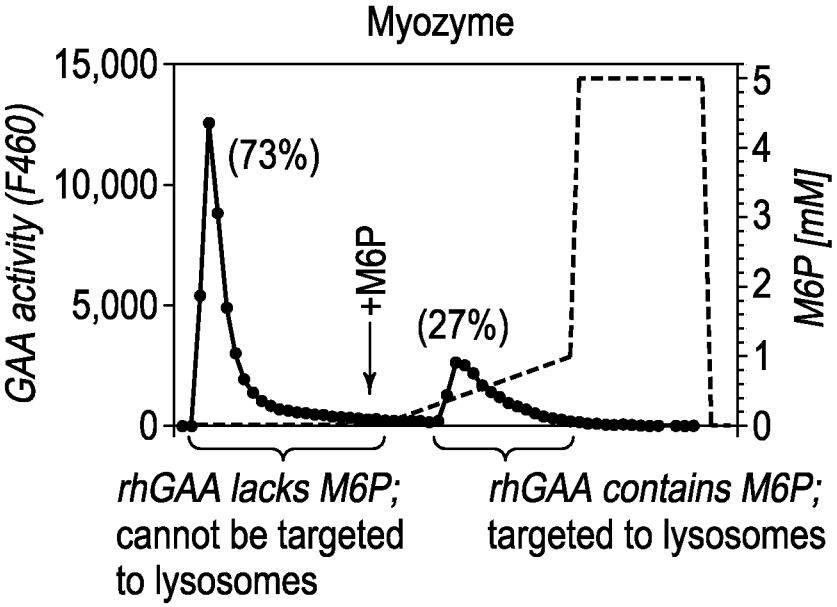

Myozyme
GAA activity (F460)
15,000
10,000
5,000
0
(73%)
+M6P
(27%)
5
4
3
2
1
0
M6P [mM]
rhGAA lacks M6P;
cannot be targeted
to lysosomes
rhGAA contains M6P;
targeted to lysosomes

Fig. 4B

ATB200 Vector Construction

- Host Cell: DG44
- Vector: pOptivec-110
  - Invitrogen vector
  - 952 aa, native signal peptide
- Screening Pressure: -HT, 500nM MTX

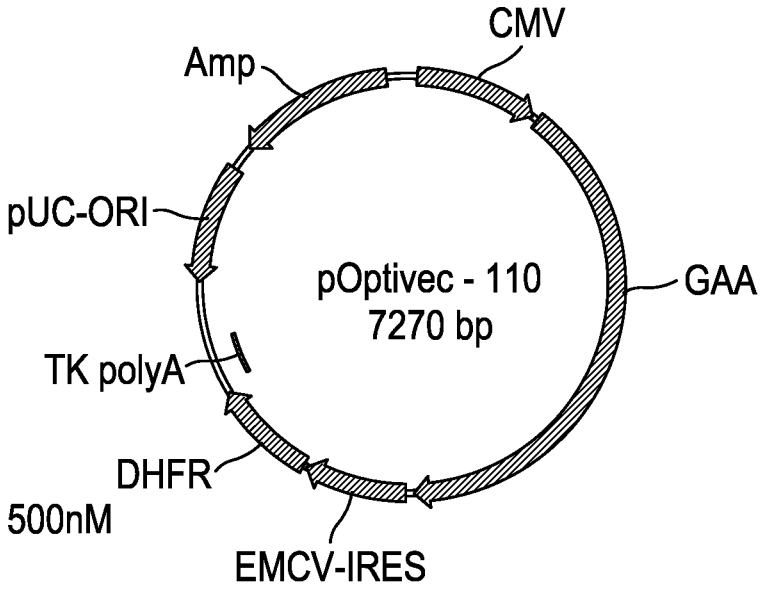


Fig. 5

CIMPR Binding Profile of Lumizyme compared to that of ATB-200 rhGAA

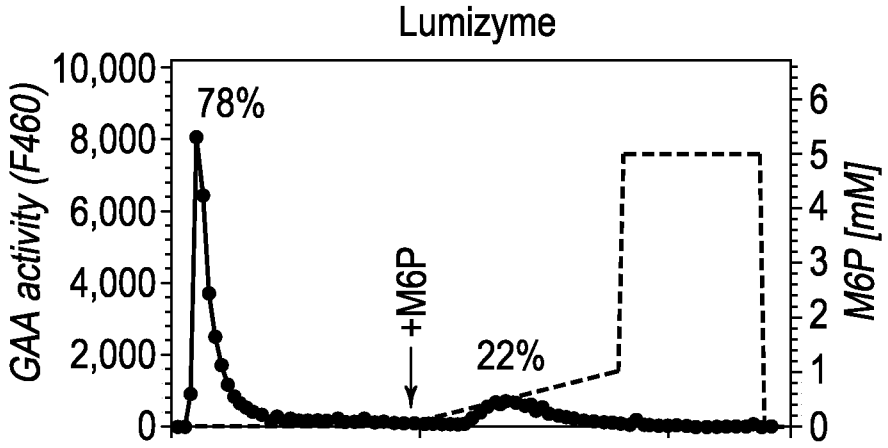


Fig. 6A

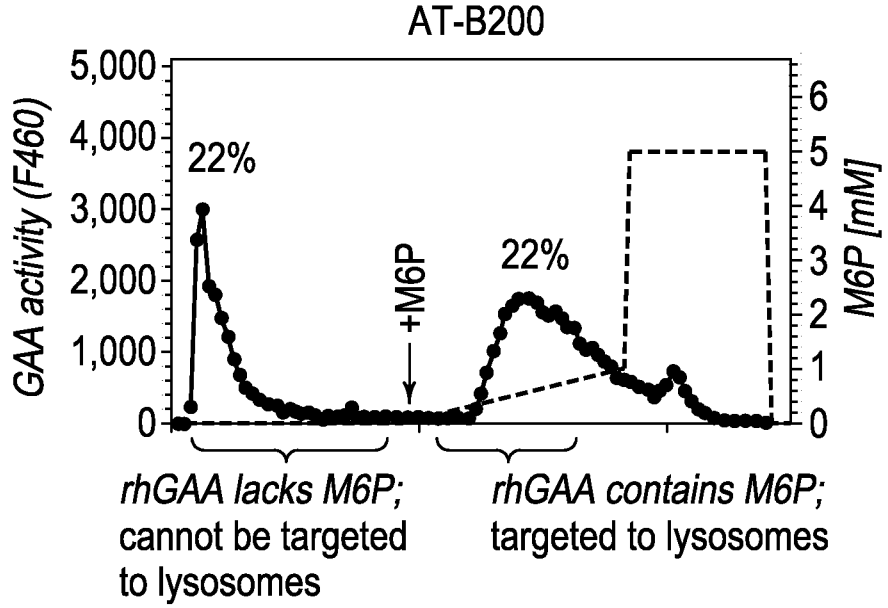


Fig. 6B

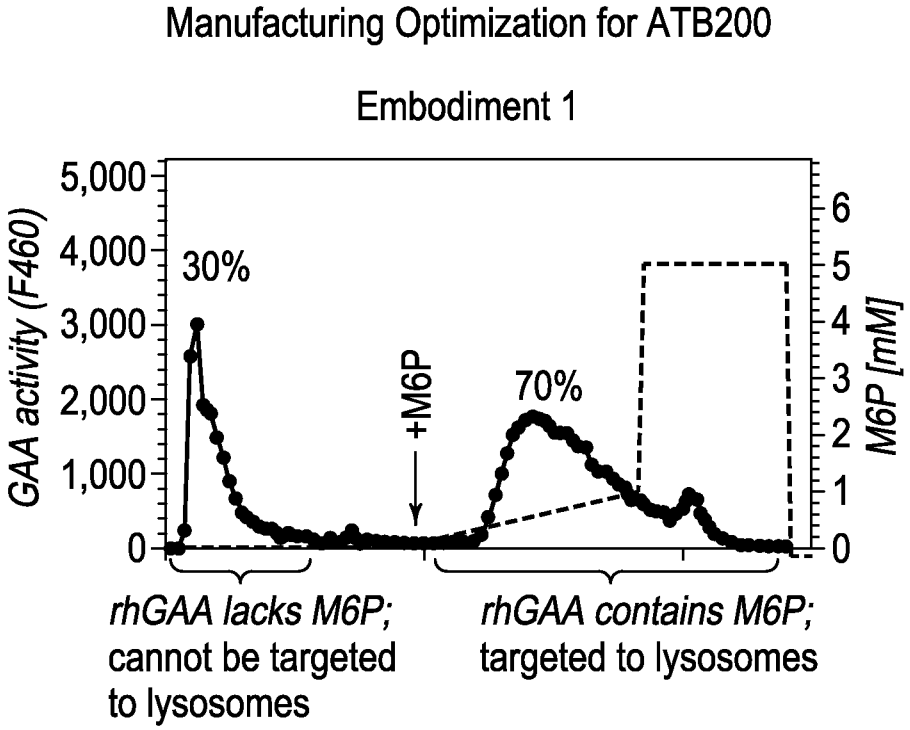

Manufacturing Optimization for ATB200
Embodiment 1
GAA activity (F460)
5,000
4,000
3,000
2,000
1,000
0
30%
+M6P
70%
6
5
4
3
2
1
0
M6P [mM]
rhGAA lacks M6P;
cannot be targeted
to lysosomes
rhGAA contains M6P;
targeted to lysosomes

Fig. 7A

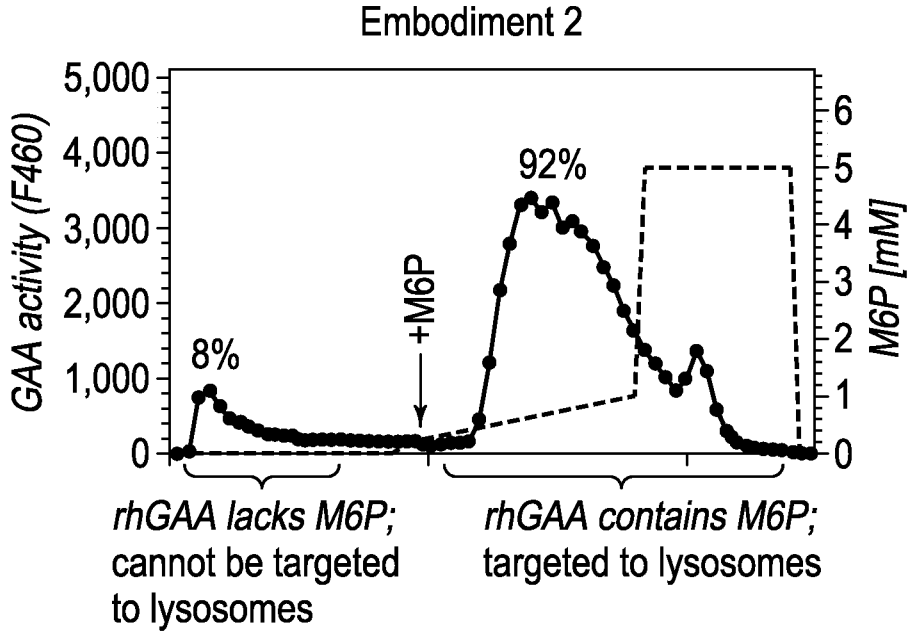
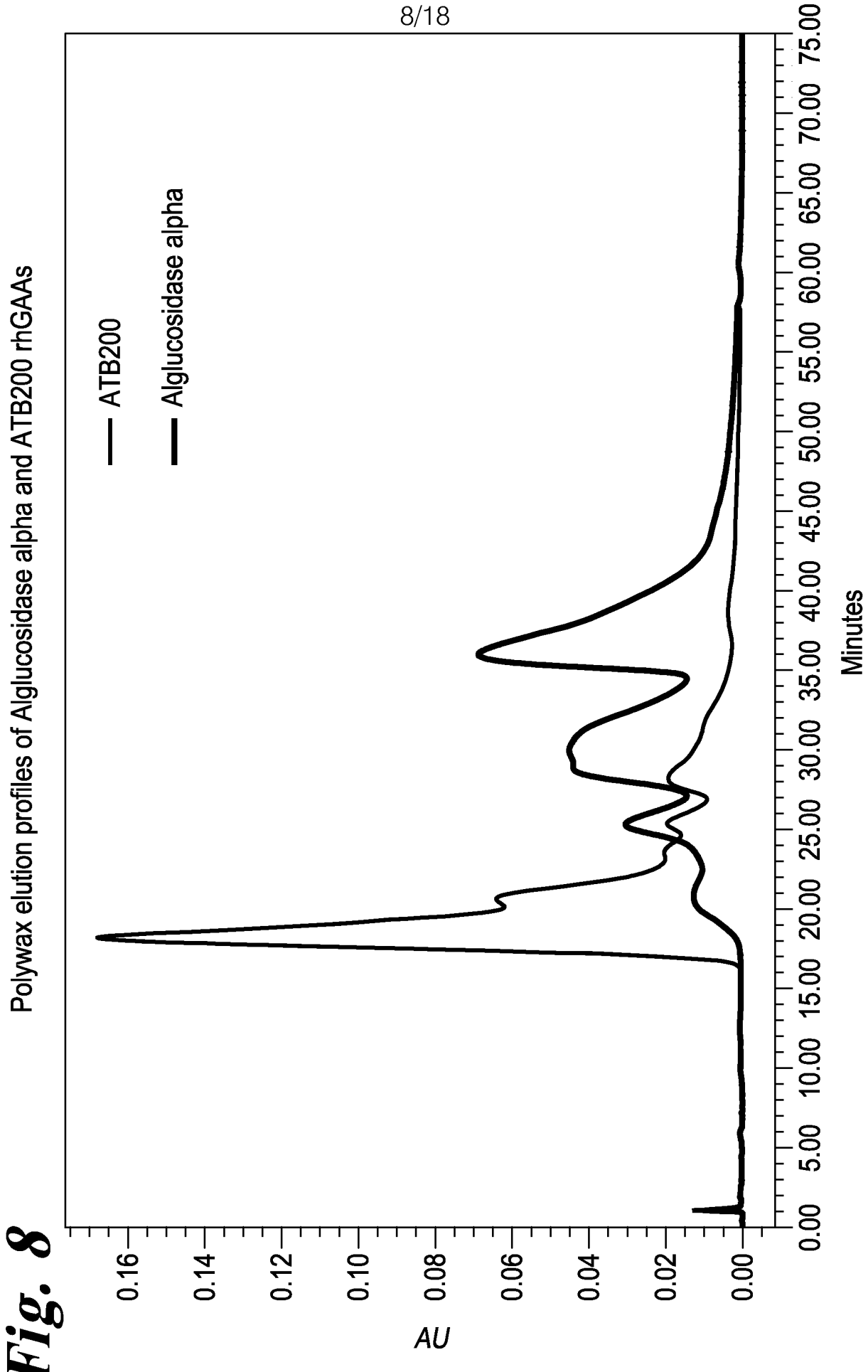

Embodiment 2
GAA activity (F460)
5,000
4,000
3,000
2,000
1,000
0
8%
+M6P
92%
6
5
4
3
2
1
0
M6P [mM]
rhGAA lacks M6P;
cannot be targeted
to lysosomes
rhGAA contains M6P;
targeted to lysosomes

Fig. 7B

Fig. 8


Polywax elution profiles of Alglucosidase alpha and ATB200 rhGAAs
ATB200
Alglucosidase alpha
AU
0.16
0.14
0.12
0.10
0.08
0.06
0.04
0.02
0.00
0.00
5.00
10.00
15.00
20.00
25.00
30.00
35.00
40.00
45.00
50.00
55.00
60.00
65.00
70.00
75.00
Minutes

Distribution of N-Glycans on rhGAA Preparations

	Lumizyme	BP-rhGAA*	ATB200	
			1	2
Complex Type N-Glycans	70.7%	48.9%	51.0%	47.5%
Hybrid Type N-Glycans	6.7%	9.7%	4.4%	3.7%
High Mannose Type N-Glycans:				
Non-phosphorylated	15.8%	23.7%	14.0%	9.9%
Mono-M6P	5.2%	10.4%	13.4%	14.2%
Bis-M6P	**1.6%**	6.8%	**17.2%**	**24.7%**

Fig. 9

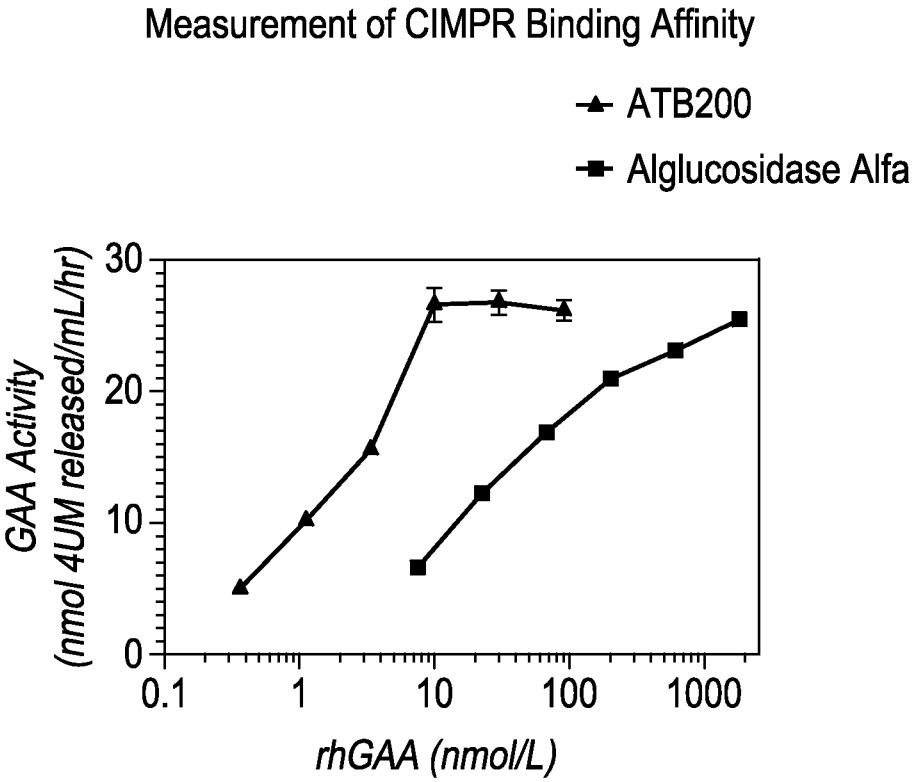


Fig. 10A

Bis-Phosphorylated Oligosaccharides Comparison

Glycan	Alglucosidase Alfa (mol bis-glycan/ mol protein)	ATB200 (mol bis-glycan/ mol protein)
Bis-M6P	0.1	1.3

Fig. 10B

CIMPR Uptake in Normal Fibroblasts

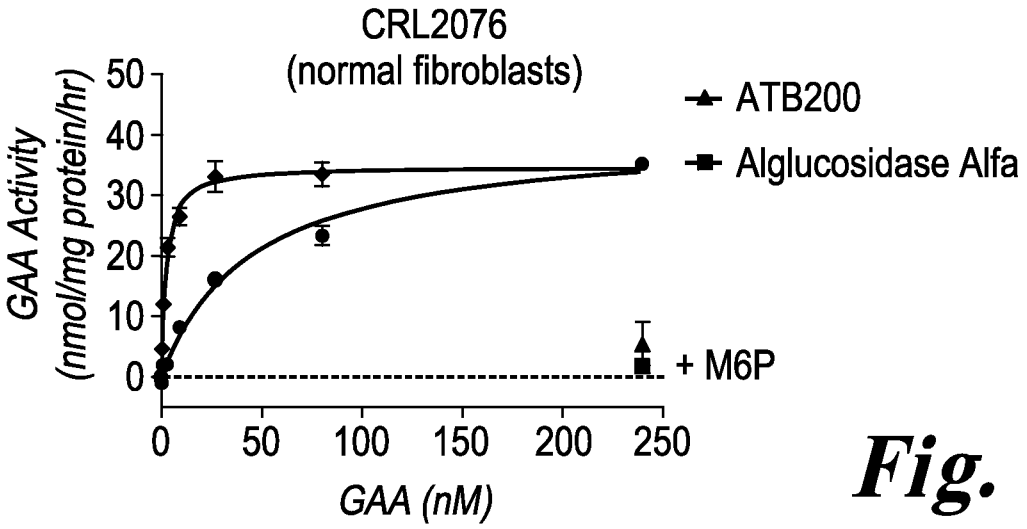


Fig. 11A

CIMPR Uptake in Pompe Fibroblasts

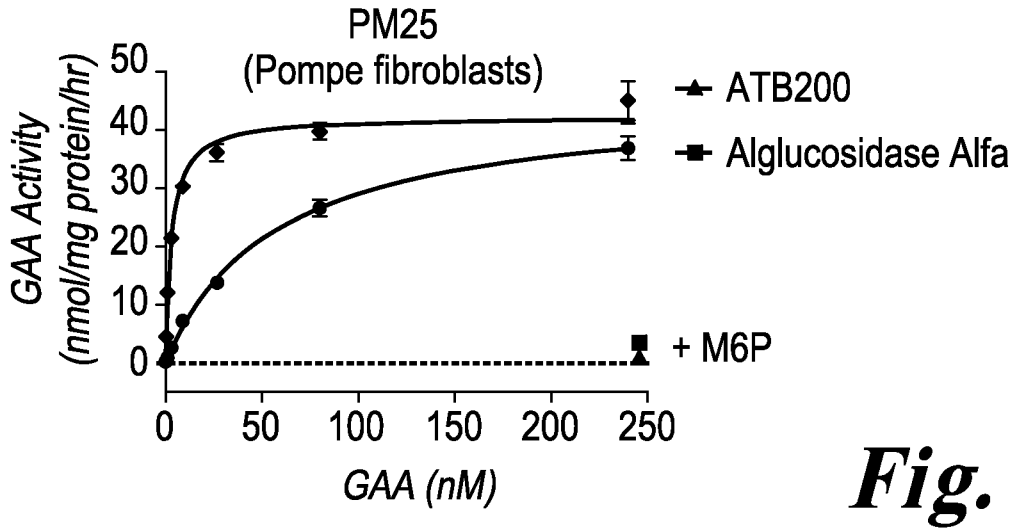


Fig. 11B

K_{uptake} Comparison in Normal and Pompe Fibroblasts

Cell Line	K_{uptake} (nM)	
	AT200	Lumizyme
normal	2	56
Pompe	3	57

Fig. 11C

Comparative glycogen clearance by ATB-200 rhGAA and Lumizyme rhAGG in Heart, Quadriceps and Tricep muscles

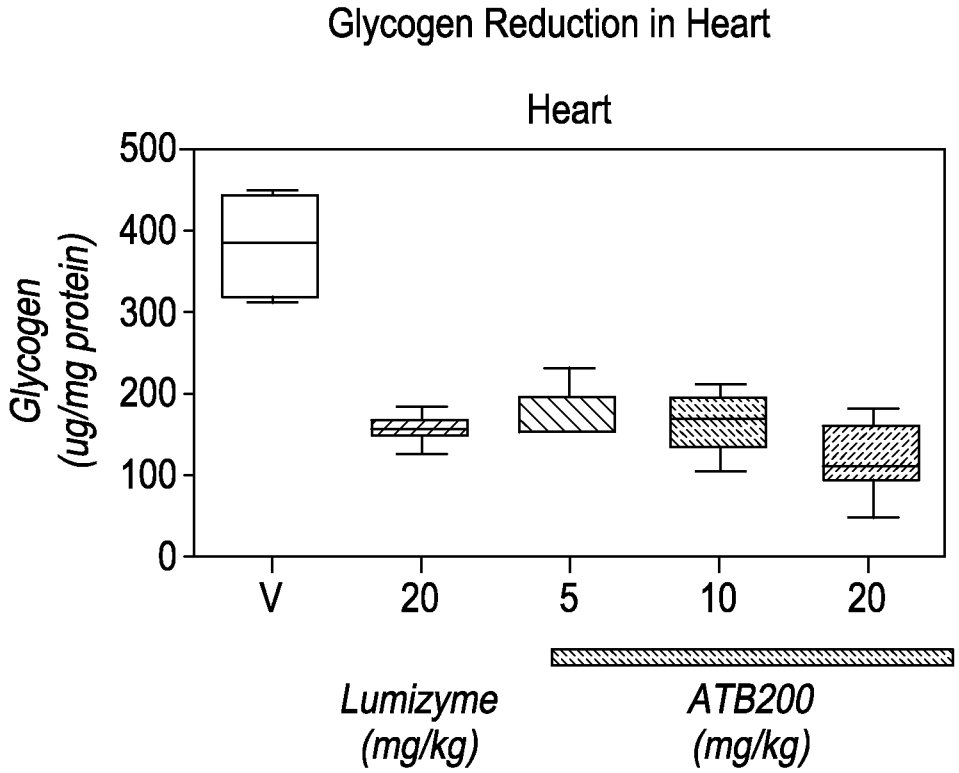


Fig. 12A

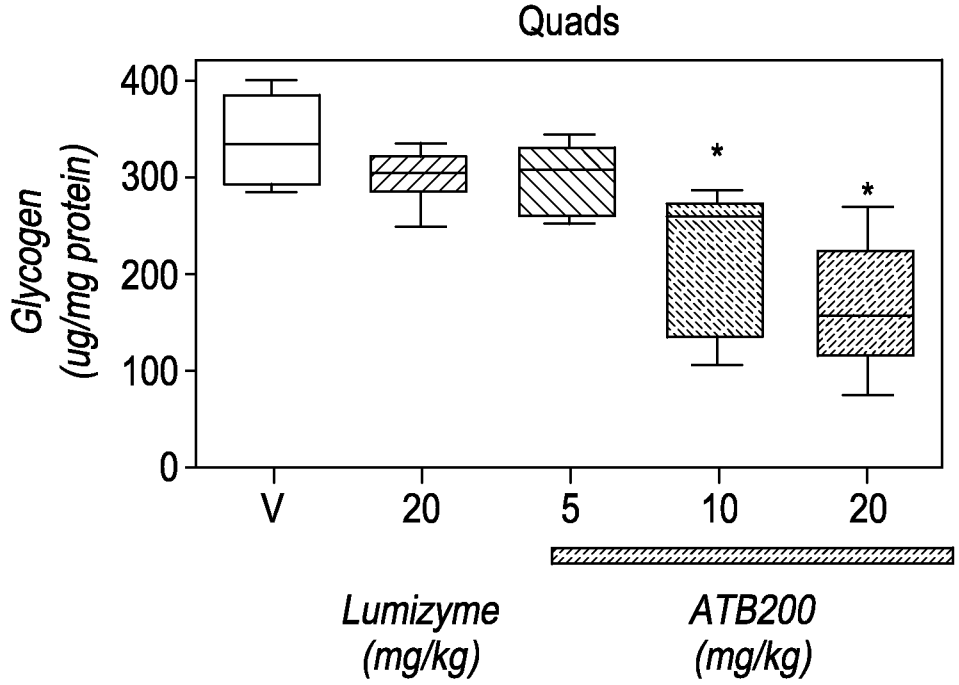


Fig. 12B

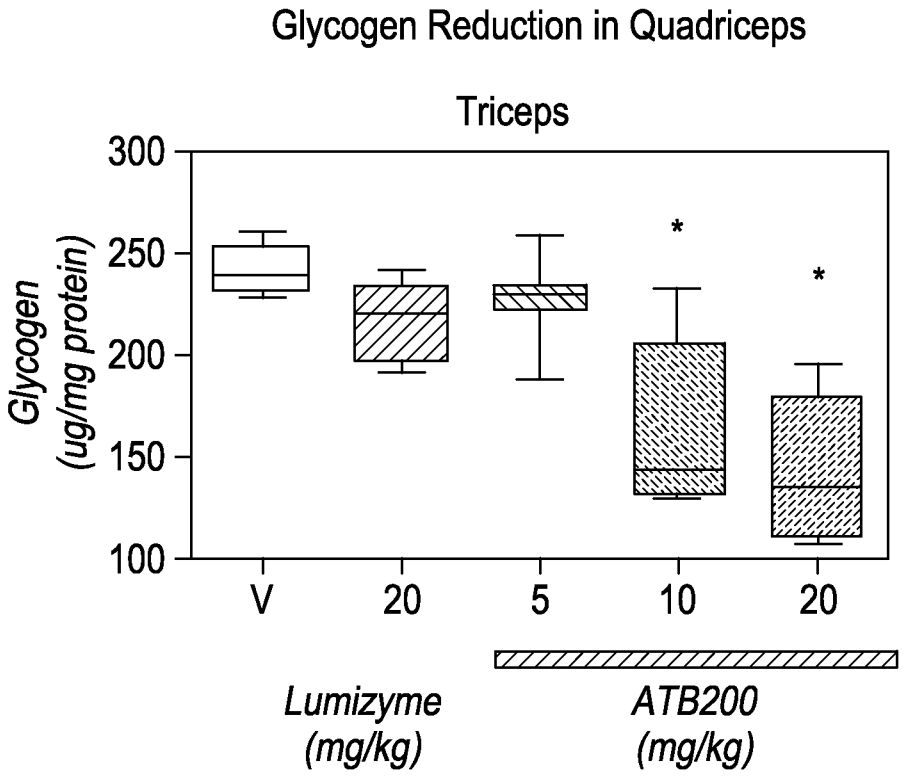

Glycogen Reduction in Quadriceps
Triceps
Glycogen (ug/mg protein)
300
250
200
150
100
V
20
5
10
20
*
*
Lumizyme (mg/kg)
ATB200 (mg/kg)

Fig. 12C

Effects of temperature on ATB-200 rhGAA folding
in presence of chaperone AT2221

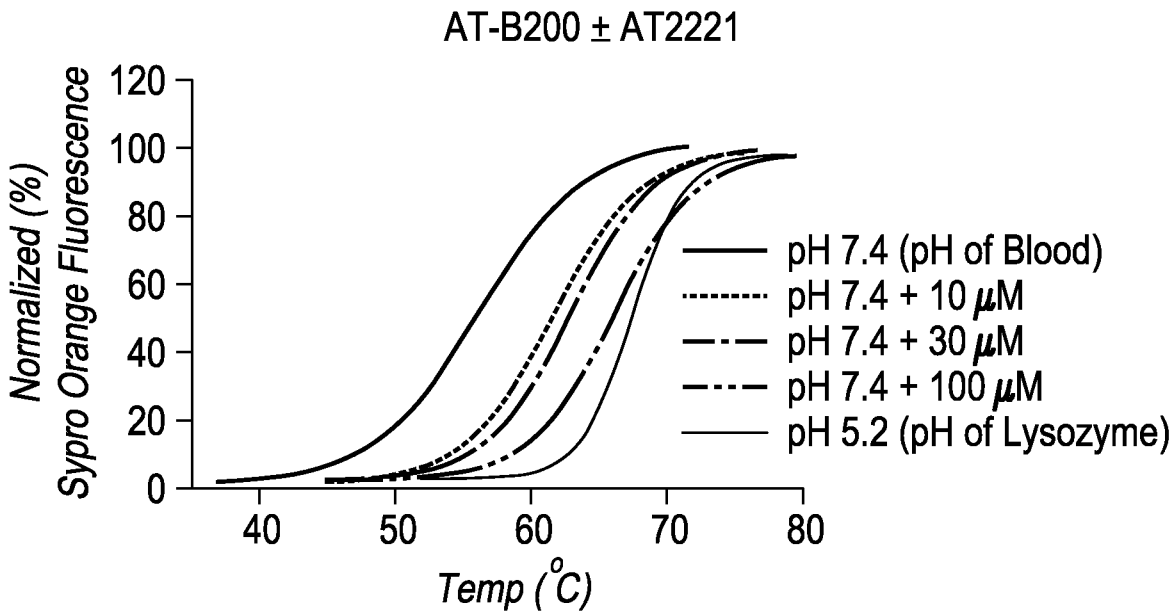


Fig. 13A

Summary of Melting Temp of ATB200 with increasing amounts of AT2221

Buffer	T_m(°C) of ATB200
pH 7.4	56.2
pH 7.4 + 10 mM AT2221	61.6
pH 7.4 +30 mM AT2221	62.9
pH 7.4 + 100 mM AT2221	66.0
pH 5.2	67.3

Fig. 13B

Comparison of % glycogen reduction in *Gaa* KO mice after Lumizyme or ATB200 administration (with or without miglustat)		
Enzyme ± Chaperone	Quadriceps	Triceps
Lumizyme alone (20 mg/Kg)	14	14
ATB200 alone (20 mg/kg)	74	62
ATB200 + Miglustat (AT2221) (20 mg/kg) + (10 mg/kg)	94	73

Fig. 14

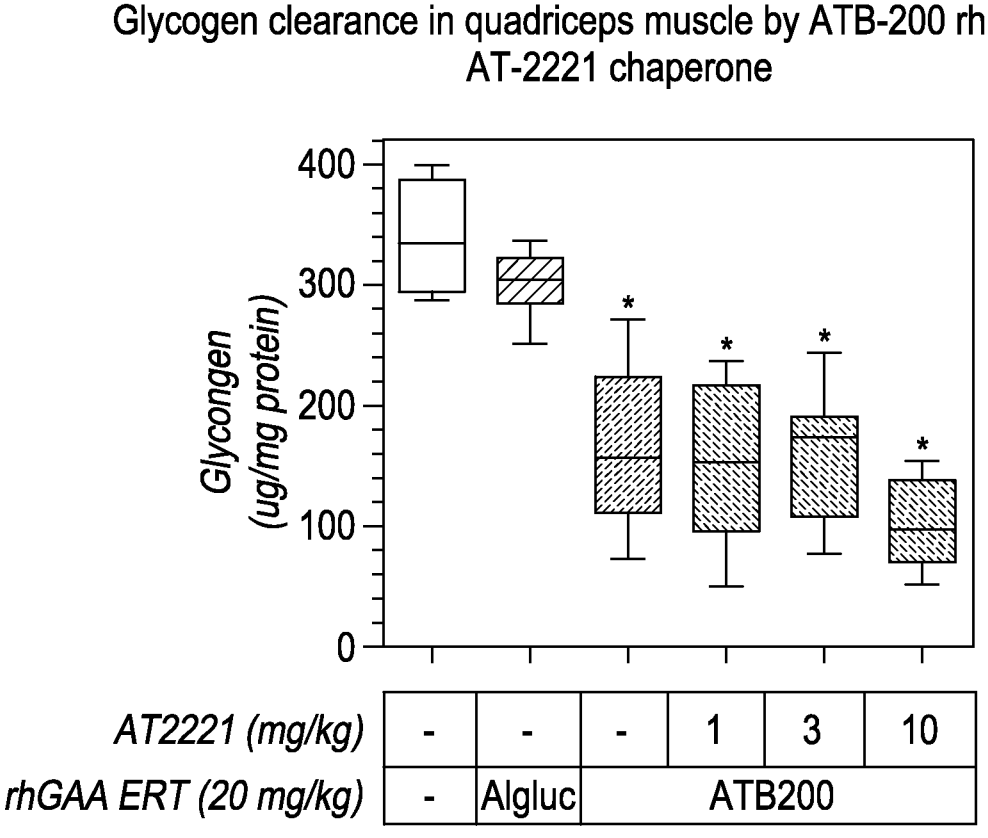


Fig. 15

PAS Glycogen staining and EM of skeletal muscle tissue from GAA KO mice treated with conventional rhGAA or ATB-200 rhGAA and AT2221

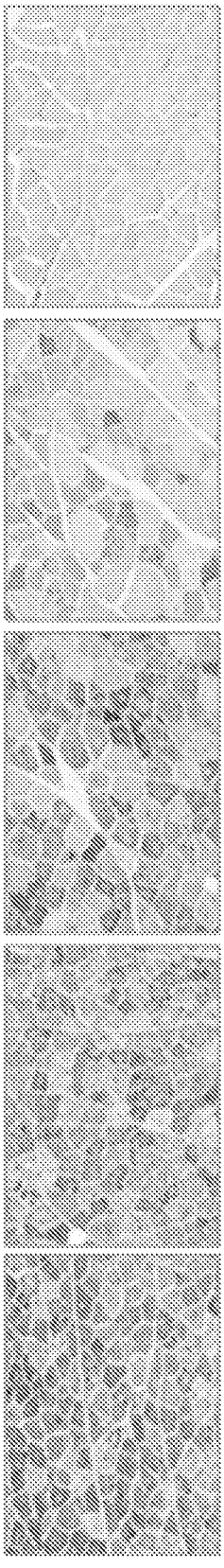


Fig.16A

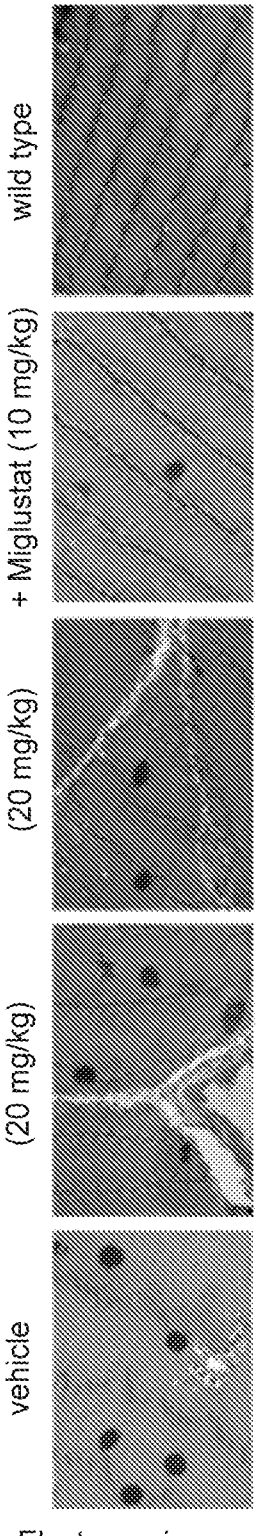


Fig.16B

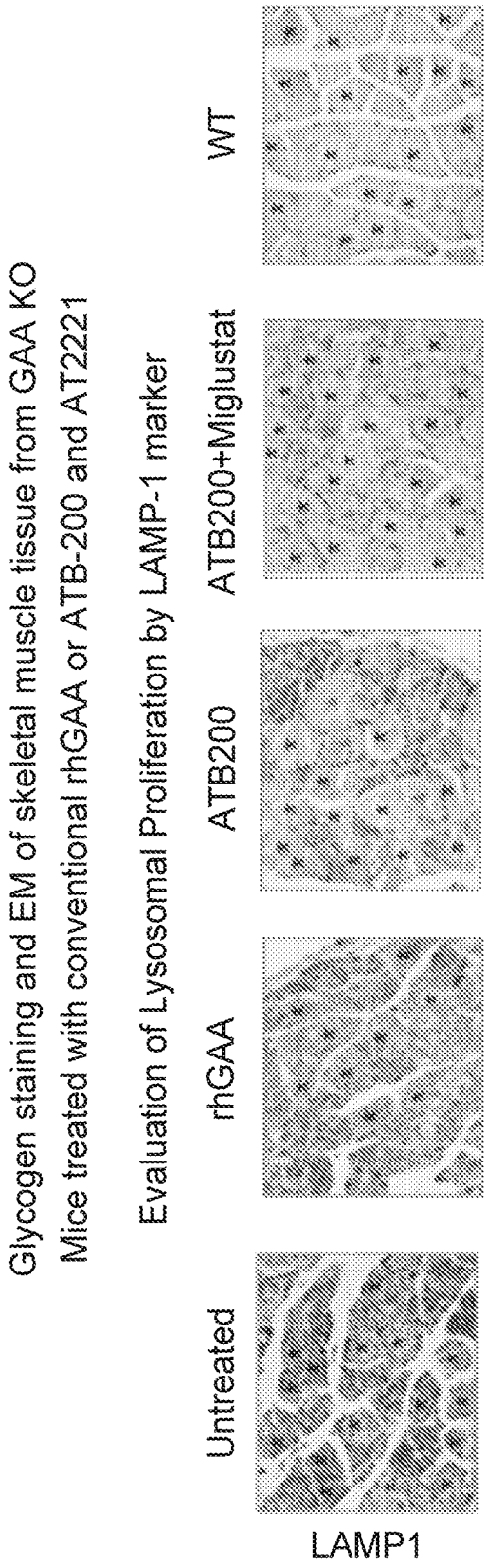


Fig.16C

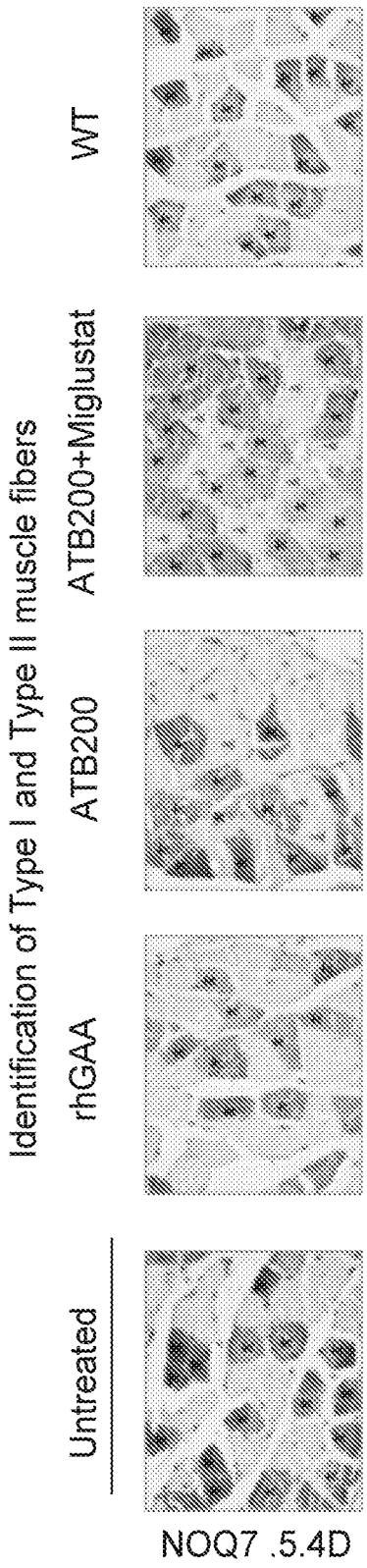


Fig.16D

PAS glycogen staining and EM of Cardiac muscle tissue from GAA KO mice treated with conventional rhGAA or ATB-200 rhGAA and Miglustate (AT-2221)

PAS Staining of Glycogen

Fig.17A

Evaluation of Lysosomal Proliferation by LAMP-1 marker

Fig.17B